

Heat Capacity and Thermodynamic Functions of $\text{Sr}(\text{La}_{1-x}\text{Ln}_x)_2\text{WO}_7$ Compounds Doped with Samarium and Europium

D.T. Sadyrbekov^{1,2}, M.R. Bissengaliyeva^{1*}, D.B. Gogol¹,
N.S. Bekturganov³, S.T. Taimassova¹

¹Institute of Problems of Complex Development of Mineral Resources, Ippodromnaya str. 5, Karaganda, Kazakhstan

²E.A. Buketov Karaganda State University, Mukanov str., 41, Karaganda, Kazakhstan

³National Academy of Sciences of the Republic of Kazakhstan, Shevchenko str. 28, Almaty, Kazakhstan

Article info

Received:
20 January 2020

Received in revised form:
30 November 2020

Accepted:
10 January 2021

Keywords:

Lanthanum; Samarium;
Europium; Tungsten;
Ternary oxide; XRD;
Adiabatic calorimetry.

Abstract

Samples based on strontium, lanthanum and tungsten with the general formula of $\text{Sr}(\text{La}_{1-x}\text{Ln}_x)_2\text{WO}_7$ doped with samarium and europium at 1 and 3 at.% were synthesized by the solid-phase method at temperatures up to 1200 °C. The crystal structure of the samples was confirmed by X-ray powder diffraction. A full-profile refinement of the structure of compounds related to monoclinic syngony with the space group $\text{P}112_1/b$ was performed. The admixture phase is a compound of the $\text{Sr}_3\text{Ln}_2\text{W}_2\text{O}_{12}$ type with a trigonal system and space group $\text{R}\bar{3}c$. Based on the results of structure refinement, the ratio of the main compound and the admixture phase in the samples was determined to introduce corrections during measurements. Using adiabatic calorimetry we measured the heat capacity of the samples and found the thermodynamic functions of main compounds over the range of 5–320 K. Anomalies were detected in the heat capacity of the samples below 15 K, and we calculated the excess and lattice heat capacity for these anomalies by means of linearization methods.

1. Introduction

Rare-earth metals are used in the production of optical materials for various purposes. Due to the transitions $4f-4f$ or $5d-4f$, they are widely used as luminophores, etc. [1].

The tungstate anion WO_4^{2-} has a tetrahedral symmetry, and the W^{6+} ion is coordinated by four O^{2-} ions. Tungstate-based luminophores are chemically more stable than sulfide-based luminophores. Tungstates intensify absorption for ultraviolet LED chips due to the charge transfer from O^{2-} to W^{6+} in the ultraviolet region [2].

In reference [3] synthesized luminophores based on strontium tungstate doped with Eu^{3+} and Sm^{3+} were investigated. The phase structure, morphology, and luminescent properties are described.

The advantage of europium compared to other dopants is its wide charge pass band in the region

close to ultraviolet radiation, a low cost, and environmental friendliness [4]. For changing the properties, for example, for increasing the fluorescence intensity in the red region, its low concentration is sufficient to increase the fluorescence intensity of a carrier in the red region [5].

Mainly, the research into the luminescent properties of SrLa_2WO_7 doped with europium [6–8] is presented in the literature, while no description of thermodynamic characteristics is available there.

This study deals with the compounds of the form $\text{Sr}(\text{La}_{1-x}\text{Sm}_x)_2\text{WO}_7$ and $\text{Sr}(\text{La}_{1-x}\text{Eu}_x)_2\text{WO}_7$, where x is 0.01, 0.03. For them, low-temperature studies of the heat capacity were carried out by adiabatic calorimetry and the main thermodynamic functions were determined. At low temperatures, abnormal deviations from the usual course of the heat capacity curve were detected, indicating the possible presence of the second-order phase transitions. The study results on the structural parameters of the synthesized samples are also presented.

*Corresponding author. E-mail: 160655@mail.ru

2. Experimental

2.1. Synthesis

Strontium carbonate SrCO_3 , tungsten oxide (VI) WO_3 , and rare-earth oxides of lanthanum La_2O_3 , samarium Sm_2O_3 , and europium Eu_2O_3 of the qualification “chemically pure” were used as starting materials for synthesizing samples designated as Sr-La(Sm)-W and Sr-La(Eu)-W. Before the synthesis rare earth metal oxides were additionally calcined at 900 °C for 2 h to remove excess moisture and absorbed carbon dioxide. A classical solid-phase method for obtaining complex oxides was used to carry out the synthesis. The weighted portions of the starting reagents, taken in stoichiometric ratios, were carefully ground in an agate mortar. Then, the resulting mixture of reagents was annealed at 700 °C for 10–12 h in the porcelain crucibles in the atmosphere of air to bind tungsten oxide.

Further, the obtained precursors were ground in an agate mortar and calcined in the alundum crucibles in the air atmosphere in three stages for 6–7 h each with a sequential increase in temperature: 6 h at 900 °C, 6 h at 1000 °C, and final annealing at 1200 °C in three steps 7 h each.

2.2. X-ray study

Experimental measurements of the diffraction patterns of the synthesized samples were carried out on a Shimadzu XRD-6000 diffractometer at room temperature (CuK_α -radiation, reflection geometry, angle range 2θ from 10° to 70°, step 0.02°). Processing of the obtained diffraction patterns, detecting known phases, and searching for isostructural compounds were carried out using the Match! Version 2.3 [9] and PDF-2 powder diffraction databases [10]. Indexing of X-ray diffraction patterns and unit cell parameters was carried out using the FullProf software package [11] and Powder Cell program [12].

2.3. Adiabatic calorimetry

The heat capacity of the obtained samples was measured from the temperature of liquid helium to 320 K by adiabatic calorimetry using a low-temperature thermophysical unit manufactured by Termax [13]. The weighed portion of the samples was 0.8–1.7 g, the measurement step was from 0.3 to 3 K depending on the temperature range, the mea-

surement interval was 4.2–320 K. In the helium temperature range, the heat capacity was measured at least twice. In the nitrogen region, the number of runs was 4–5 or more times.

3. Results and discussion

X-ray phase analysis of the synthesized samples carried out using Match! and the PDF-2 database showed that the composition of all the samples besides the main phase isostructural to the compound SrLa_2WO_7 [14] (PDF-2 No.00-049-0353), includes a certain amount of another phase isostructural to the compound $\text{Sr}_3\text{Re}_2\text{O}_{12}$ [15] (PDF-2 No. 01-081-1481). Taking into account the elements available in the synthesized samples, the composition of the admixture phase can be represented as $\text{Sr}_3\text{Ln}_2\text{W}_2\text{O}_{12}$.

To refine the parameters of the crystal structure of the obtained compounds and determine the phase ratio in the samples, a full-profile analysis of the experimental diffraction patterns was carried out. The calculation results are given in Fig. 1.

While making calculations, we got rather low values of the discrepancy factors (Table 1). Table 1 also shows the unit cell parameters of the compounds entering into the composition of the compounds and the phase ratios resulted from the refinement. Thus, based on the results of the measurements carried out by X-ray diffraction and calculations made by the full-profile analysis, we confirmed a formation of the target compounds, obtained the refined values of the compound crystal structure parameters and determined the ratio of the target and side phases in the samples, which was used to introduce corrections to the results of calorimetric measurements.

The heat capacity correction on the admixture content in the samples was made as follows. The heat capacity of the $\text{Sr}_3\text{Ln}_2\text{W}_2\text{O}_{12}$ compound was calculated as the sum of the heat capacities of La_2O_3 [16], Sm_2O_3 [17], SrO [18], and SrWO_4 [19] in the corresponding ratios. The calculated values of the heat capacities from [19] correlate well with the experimental data presented in [20]. The specific heat of the $\text{Sr}_3\text{Ln}_2\text{W}_2\text{O}_{12}$ compound in proportion to its mass fraction was subtracted from the total experimentally measured the specific heat of the samples. The reliability of the introduced correction is confirmed by the proximity of the specific heat values of the samples studied to the specific heat of the undoped SrLa_2WO_7 compound [21].

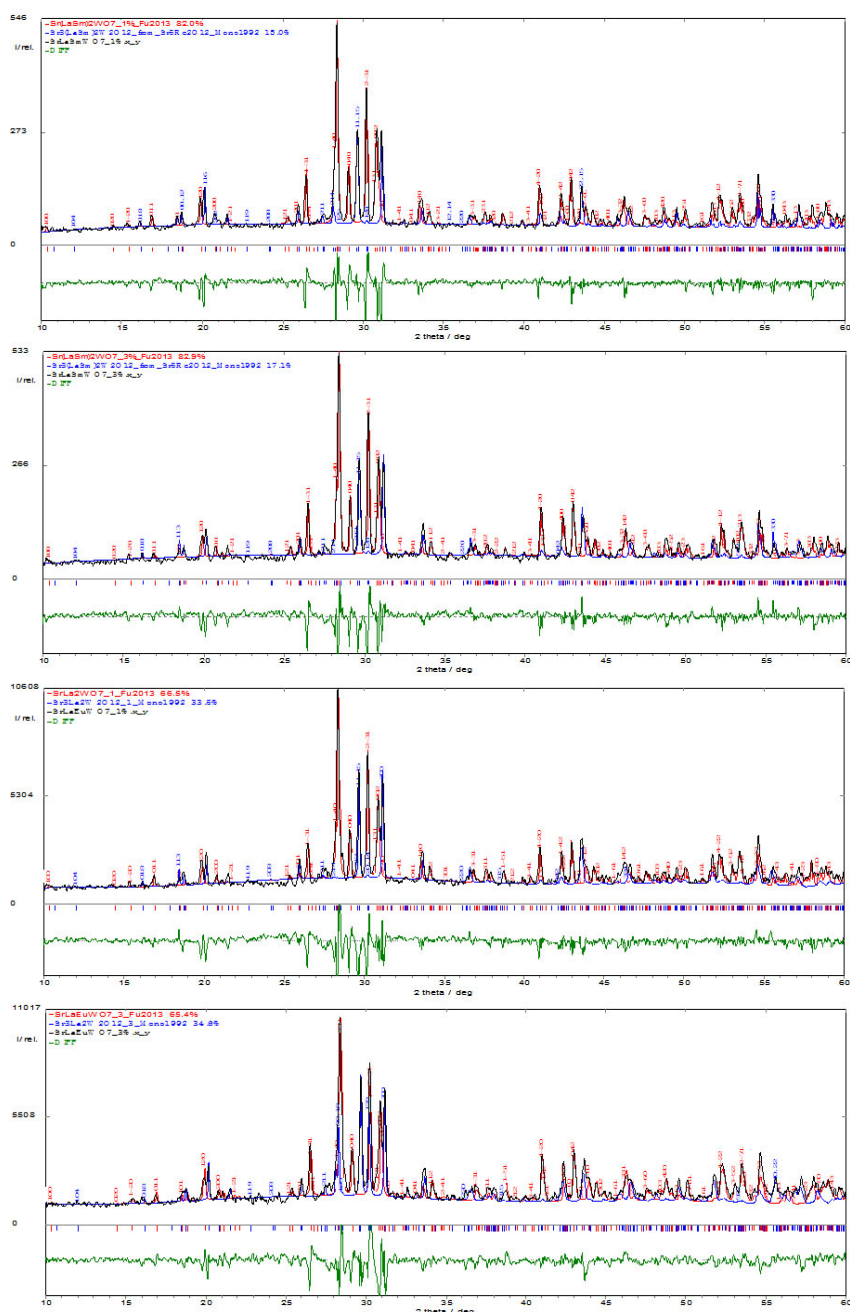


Fig. 1. Experimental, theoretical, and difference diffraction patterns of the synthesized samples. From top to bottom: Sr-La(Sm)-W(1%), Sr-La(Sm)-W(3%), Sr-La(Eu)-W(1%), Sr-La(Eu)-W(3%). The vertical strokes mark Bragg's positions.

Table 1
Results of a full-profile analysis of the samples

Sample	Basic phase $\text{Sr}(\text{La}_{1-x}\text{Ln}_x)_2\text{WO}_7$ parameters (space group $\text{P}112_1/\text{b}$)				Admixture phase parameters (space group $\text{R}\bar{3}\text{c}$)		Discrepancy factors		Phase ratio, mass%
	a, Å	b, Å	c, Å	γ , deg	a, Å	c, Å	R_p	R_{wp}	
Sr-La(Sm)-W(1%)	8.8303	12.6780	5.7890	105.123	9.9158	56.6986	9.29	13.28	81.01:18.99
Sr-La(Sm)-W(3%)	8.8304	12.6804	5.7772	105.116	9.9269	56.7018	11.28	15.79	82.90:17.10
Sr-La(Eu)-W(1%)	8.8274	12.6750	5.7818	105.147	9.9292	56.6129	10.84	15.27	66.54:33.46
Sr-La(Eu)-W(3%)	8.8274	12.6780	5.7757	105.142	9.9329	56.6545	9.47	12.82	65.38:34.62

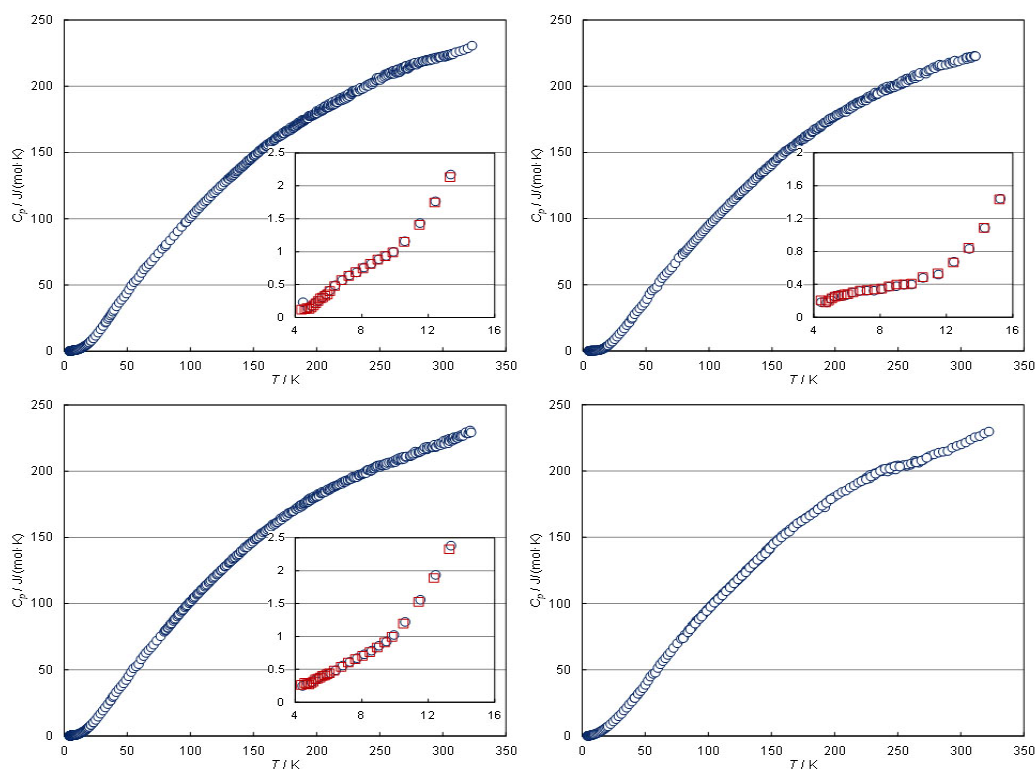


Fig 2. Experimental molar heat capacity of the synthesized compounds: top left Sr(La_{0.99}Sm_{0.01})₂WO₇, bottom left Sr(La_{0.97}Sm_{0.03})₂WO₇, top right Sr(La_{0.99}Eu_{0.01})₂WO₇, bottom right Sr(La_{0.97}Eu_{0.03})₂WO₇.

The heat capacity of the Sr-La(Eu)-W(3%) sample was experimentally measured from 40 K. To calculate the values of thermodynamic functions of the compound over the entire temperature range, its heat capacity was extrapolated to absolute zero by the method described in reference [22], by the equation:

$$C(T) = (AT^{-1/\alpha\beta} + 1)^{-1/\alpha}.$$

This equation approximates well both the low-temperature and high-temperature branches of the heat capacity and can be used to describe the heat capacity of a fairly wide range of solids [23].

The results of experimental measurements of the heat capacity of the samples are presented in Fig. 2.

In the samples measured from the temperature of liquid helium, we detected anomalies of the specific heat at low temperatures associated with the presence of Sm³⁺ and Eu³⁺ ions in the crystal structure of the compounds. The anomalies have the form of gentle blurry peaks of low intensity in the range from 5 to 8 K. To determine an excess anomalous contribution, the lattice component of the specific heat was determined by the equations [24, 25]:

$$\frac{C_L}{T^3} = K \left(1 - \frac{C_L}{3Rn}\right)^m$$

$$\ln\left(\frac{C_L}{T^3}\right) = m \ln\left(1 - \frac{C_L}{3Rn}\right) + \ln K.$$

The linear areas of the dependences used to find the lattice component of the specific heat of the samples studied are presented in Fig. 3.

The dependences presented in Fig. 4 were obtained for the calculated lattice and anomalous heat capacity components. The equations of these dependences were used to calculate the changes in the enthalpy and entropy in the anomalous transitions observed.

As a rule, for mathematical calculation and simulation of the thermodynamic characteristics of low-temperature anomalies of this kind, the Schottky equation is used. It relates the number of possible energy levels in the compound, the energy value for these levels, and the population of the levels by the particles of a substance involved in the phase transformation as applied to one mole of the amount of the substance. However, since the observed anomalies are caused by the presence of the dopant atoms of lanthanide, the number of which

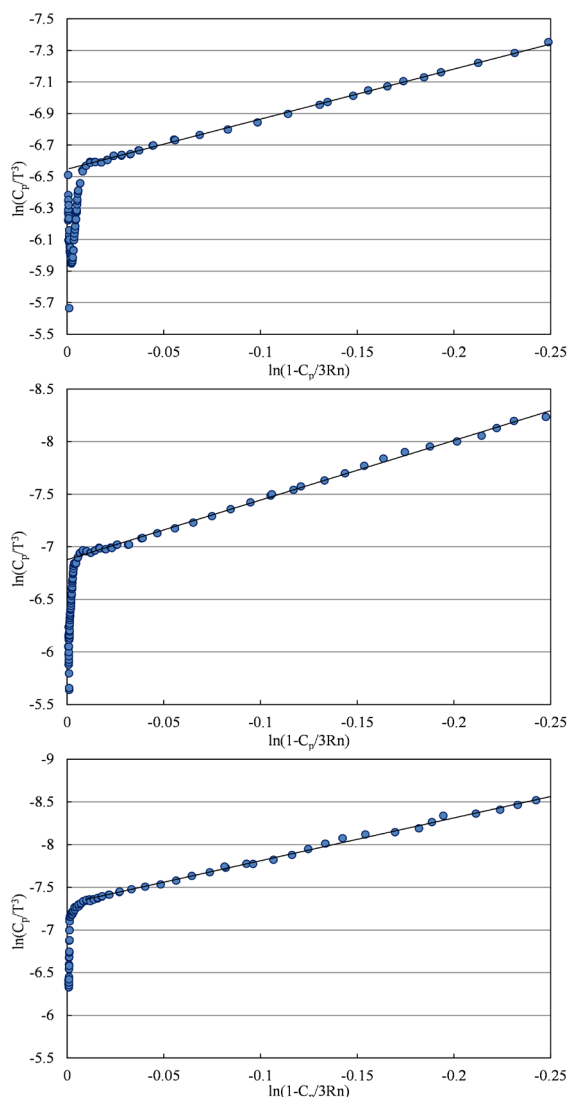


Fig. 3. Linearized heat capacity of the samples, from top to bottom: $\text{Sr}(\text{La}_{0.99}\text{Sm}_{0.01})_2\text{WO}_7$, $\text{Sr}(\text{La}_{0.97}\text{Sm}_{0.03})_2\text{WO}_7$, $\text{Sr}(\text{La}_{0.99}\text{Eu}_{0.01})_2\text{WO}_7$.

is hundredths fractions of a mole, this equation was not applied. Instead, a mathematical equation for the asymmetric normal distribution describing the dependencies observed with acceptable accuracy was used. The obtained values of changes in the enthalpy and entropy in the anomalies of the heat capacity of the samples are presented in Table 2.

Table 2

Magnitudes of change of the enthalpy and changes of entropy in the anomalous heat capacity of the samples

Sample	ΔH_{an} , J/mol	ΔS_{an} , J/(mol·K)
$\text{Sr}(\text{La}_{0.99}\text{Sm}_{0.01})_2\text{WO}_7$	1.12 ± 0.22	0.154 ± 0.031
$\text{Sr}(\text{La}_{0.97}\text{Sm}_{0.03})_2\text{WO}_7$	1.02 ± 0.21	0.165 ± 0.033
$\text{Sr}(\text{La}_{0.99}\text{Eu}_{0.01})_2\text{WO}_7$	0.62 ± 0.16	0.099 ± 0.025

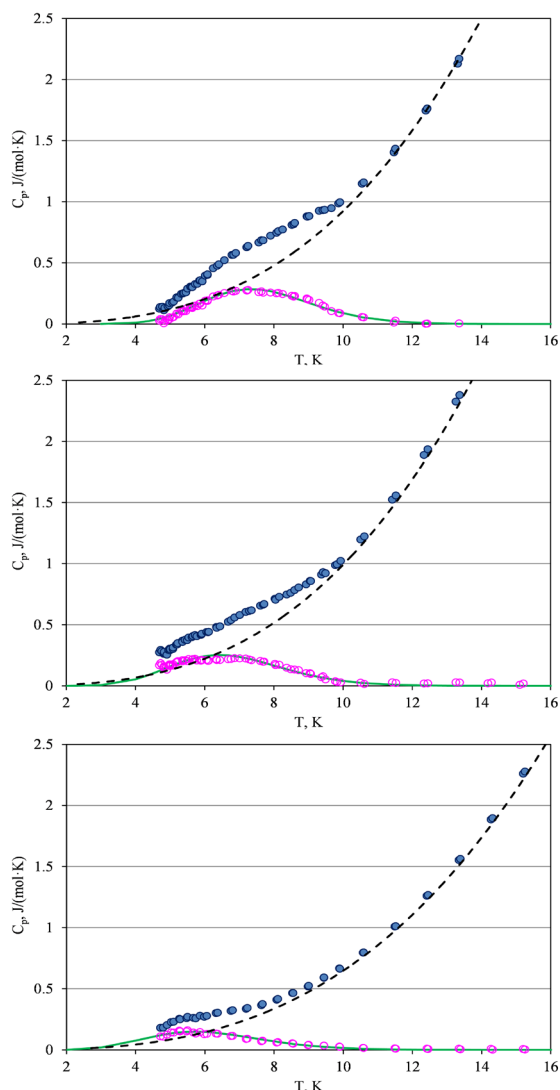


Fig. 4. Total, lattice and abnormal heat capacity of the samples, from top to bottom: $\text{Sr}(\text{La}_{0.99}\text{Sm}_{0.01})_2\text{WO}_7$, $\text{Sr}(\text{La}_{0.97}\text{Sm}_{0.03})_2\text{WO}_7$, $\text{Sr}(\text{La}_{0.99}\text{Eu}_{0.01})_2\text{WO}_7$.

The magnitude of the entropy change in the observed transformations is much less than a theoretical value of $R \ln 2$, which is due to the replacement of only a part of the lanthanum atoms by the atoms of samarium and europium upon doping the compounds.

To calculate the thermodynamic functions, a mathematical description of the temperature dependences of the heat capacity of the compounds obtained was carried out. When processing the measured data, a spline approximation of the experimental heat capacity values by the third degree polynomials of the form $C_p = a_0 + a_1T + a_2T^2 + a_3T^3$ was used. Below 5 K, the heat capacity values are extrapolated to absolute zero in accordance with an odd degree polynomial $C_p = aT^3 + bT^5$. The overlap of the experimental points in the polynomial change regions was at least 3–4 points.

Based on the smoothed heat capacity values, the corridor of measurement errors of the experimental points within the 95% confidence interval is determined. The error was found as the ratio of the difference between the experimental measurement and its smoothed value to the value of the smoothed value. The scatter of the experimental points relative to the smoothed curves is shown in Fig. 5, where the dashed lines indicate the boundaries of the 95% confidence interval.

The values of the basic thermodynamic functions of the entropy $S(T)$, change of the enthalpy $H(T) - H(0)$, and the reduced thermodynamic potential $\Phi(T)$ of the synthesized samples were determined by the coefficients of the obtained polynomials by the following expressions:

$$S_T^\circ = \int_0^T \frac{C_p}{T} dT = a_0 \ln T + \sum_{n=1}^3 \frac{a_n T^n}{n}$$

$$H_T^\circ - H_0^\circ = \int_0^T C_p dT = \sum_{n=0}^3 \frac{a_n T^{n+1}}{n+1},$$

$$\Phi_T^* = S_T^\circ - \frac{\Delta H_T^\circ}{T}.$$

The calculated values of the thermodynamic functions of the compounds studied over the temperature range of 5–300 K are presented in Table 3 together with the corresponding errors.

4. Conclusion

For the samples Sr(La_{1-x}Sm_x)₂WO₇ and Sr(La_{1-x}Eu_x)₂WO₇ synthesized by the solid-state method, their crystal structure was confirmed and their thermodynamic functions in the range of 5–320 K were investigated. The anomalies associated with the presence of lanthanide atoms in the structure of the compounds were detected in the low-temperature heat capacity of the samples. Due to rather large errors while calculating the excess component, the found values of changing in the entropy and enthalpy in the anomalies do not have a pronounced dependence on the content of the dopant element. The nature of the anomalies detected is the subject of further research.

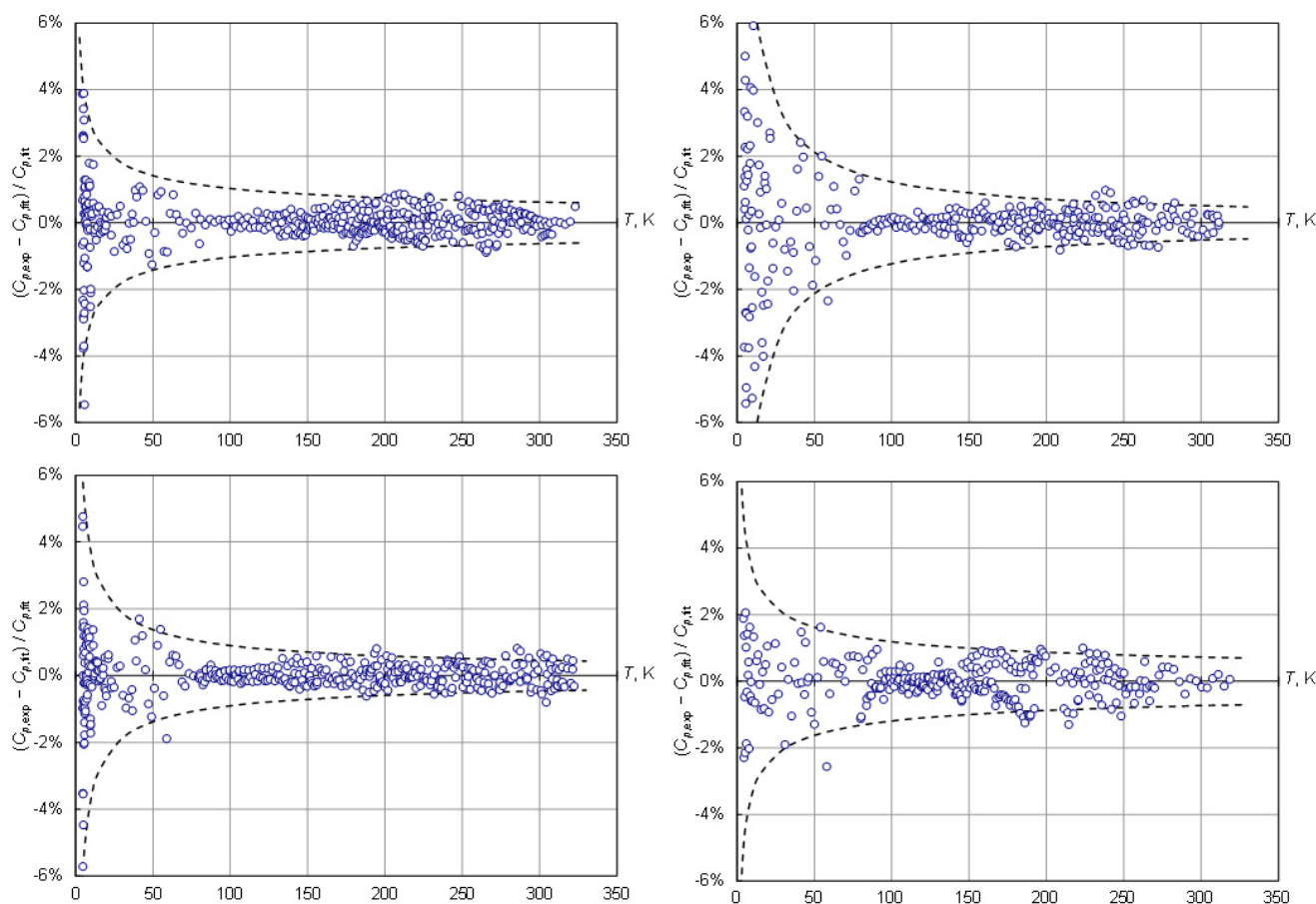


Fig. 5. Deviations of the experimental values of the specific heat of the samples: top left Sr(La_{0.99}Sm_{0.01})₂WO₇, bottom left Sr(La_{0.97}Sm_{0.03})₂WO₇, top right Sr(La_{0.99}Eu_{0.01})₂WO₇, bottom right Sr(La_{0.97}Eu_{0.03})₂WO₇.

Table 3
Thermodynamic functions of the compounds $\text{Sr}(\text{La}_{1-x}\text{Ln}_x)_2\text{WO}_7$

T, K	$\text{Sr}(\text{La}_{0.99}\text{Sm}_{0.01})_2\text{WO}_7$			$\text{Sr}(\text{La}_{0.99}\text{Sm}_{0.03})_2\text{WO}_7$			$\text{Sr}(\text{La}_{0.99}\text{Eu}_{0.01})_2\text{WO}_7$			$\text{Sr}(\text{La}_{0.97}\text{Eu}_{0.03})_2\text{WO}_7$					
	$C_p^\circ(T)$, J/mol·K	$S^\circ(T)$, J/mol·K	$\Delta H^\circ(T)$ J/mol	$C_p^\circ(T)$, J/mol·K	$S^\circ(T)$, J/mol·K	$\Delta H^\circ(T)$ J/mol	$C_p^\circ(T)$, J/mol·K	$S^\circ(T)$, J/mol·K	$\Delta H^\circ(T)$ J/mol	$C_p^\circ(T)$, J/mol·K	$S^\circ(T)$, J/mol·K	$\Delta H^\circ(T)$ J/mol			
5	0.168	0.050	0.192	0.011	0.140	0.478	0.044	0.215	0.067	0.257	0.016	0.227	0.084	0.307	0.023
10	1.032	0.459	3.386	0.121	0.559	3.703	0.189	0.425	0.290	1.916	0.099	1.393	0.516	3.776	0.138
15	2.998	1.186	12.69	0.341	1.349	13.81	0.428	1.338	0.573	5.538	0.204	3.662	1.471	15.94	0.409
20	6.588	2.504	36.02	0.703	2.770	38.96	0.822	4.348	1.326	18.99	0.377	6.981	2.959	42.20	0.850
25	11.67	4.491	81.00	1.251	4.879	86.71	1.411	8.785	2.755	51.42	0.698	11.09	4.944	87.05	1.462
30	17.90	7.156	154.6	2.004	7.641	162.9	2.211	14.05	4.813	108.3	1.205	15.89	7.382	154.3	2.240
35	24.64	10.43	261.2	2.968	10.95	270.7	3.218	19.90	7.425	193.4	1.901	21.25	10.24	247.3	3.174
40	31.36	14.16	401.2	4.130	14.66	409.8	4.412	25.83	10.47	307.6	2.778	26.65	13.43	367.0	4.254
45	38.12	18.24	574.9	5.468	18.67	580.5	5.771	32.04	13.86	452.1	3.818	32.40	16.89	514.4	5.463
50	44.84	22.61	782.4	6.962	22.94	783.5	7.273	38.60	17.58	628.5	5.005	38.76	20.63	692.0	6.791
60	57.30	31.90	1294	10.34	32.07	1286	10.64	51.19	25.74	1078	7.769	51.42	28.84	1144	9.771
70	68.73	41.60	1924	14.10	41.66	1910	14.38	62.92	34.52	1649	10.96	63.22	37.67	1718	13.12
80	79.54	51.48	2666	18.16	51.50	2647	18.40	73.98	43.65	2334	14.47	74.53	46.85	2407	16.76
90	90.30	61.47	3515	22.42	61.49	3497	22.63	84.60	52.98	3127	18.23	85.55	56.27	3208	20.62
100	101.1	71.56	4473	26.82	71.61	4459	27.03	94.98	62.43	4026	22.18	95.87	65.83	4116	24.67
110	111.2	81.67	5535	31.35	81.75	5523	31.54	104.9	71.95	5025	26.27	105.6	75.42	5124	28.84
120	120.7	91.76	6695	35.96	91.86	6685	36.15	114.4	81.49	6122	30.47	115.0	85.01	6227	33.13
130	129.8	101.8	7948	40.64	101.9	7940	40.82	123.6	91.01	7313	34.76	124.3	94.58	7423	37.49
140	138.3	111.7	9289	45.36	111.9	9286	45.54	132.7	100.5	8594	39.12	133.6	104.1	8712	41.90
150	147.0	121.6	10716	50.12	121.7	10718	50.29	141.5	110.0	9966	43.53	142.9	113.7	10096	46.37
160	154.8	131.3	12226	54.89	131.5	12231	55.06	149.5	119.4	11422	47.98	151.1	123.2	11566	50.88
170	161.8	140.9	13810	59.66	141.1	13819	59.84	157.1	128.7	12955	52.45	158.6	132.6	13115	55.40
180	168.2	150.3	15460	64.44	150.6	15477	64.62	164.1	137.8	14562	56.94	165.6	141.8	14736	59.95
190	174.2	159.6	17172	69.21	159.9	17201	69.39	170.8	146.9	16236	61.43	172.5	151.0	16427	64.50
200	179.8	168.7	18943	73.95	169.1	18984	74.15	177.1	155.8	17976	65.93	179.3	160.0	18185	69.05
210	185.1	177.6	20768	78.68	178.0	20821	78.88	182.7	164.6	19776	70.42	185.8	168.9	20015	73.59
220	190.4	186.3	22645	83.37	186.8	22707	83.59	187.9	173.2	21629	74.90	191.3	177.7	21900	78.12
230	195.4	194.9	24574	88.03	195.4	24640	88.26	192.7	181.7	23532	79.36	196.3	186.3	23839	82.64
240	200.3	203.3	26553	92.66	203.8	26618	92.90	197.2	190.0	25482	83.79	200.5	194.7	25823	87.13
250	205.0	211.6	28580	97.25	212.0	28636	97.50	201.5	198.1	27475	88.20	203.7	203.0	27846	91.60
260	209.4	219.7	30652	101.8	220.1	30690	102.1	205.6	206.1	29511	92.58	205.6	211.0	29894	96.04
270	213.9	227.7	32773	106.3	228.0	32777	106.6	210.0	213.9	31590	96.93	208.5	218.8	31963	100.4
273.15	215.0	230.2	33449	107.7	230.4	33443	108.0	211.3	216.4	32253	98.30	209.6	221.3	32621	101.8
280	217.1	235.5	34929	110.8	235.7	34901	111.1	213.9	221.6	33710	101.3	212.1	226.5	34066	104.8
290	219.9	243.2	37114	115.2	243.3	37060	115.5	217.2	229.2	35865	105.5	216.1	234.0	36206	109.1
298.15	222.1±1.4	249.3±2.3	38916±312	118.8±2.1	249.4±2.0	38845±253	119.1±1.7	219.5±1.1	235.3±2.5	37645±304	109.0±2.0	219.5±1.6	240.0±2.6	37981±351	112.6±2.3
300	222.6	393.27	39327	119.6	221.2	39254	119.9	220.0	236.6	38051	109.8	220.2	241.4	38388	113.4

Acknowledgment

This research has been funded by the Science Committee of the Ministry of Education and Science of the Republic of Kazakhstan (grant number AP09259070).

References

- [1]. N.P. Sabalisk, F. Lahoz, M.C. González-Silgo, J.D. Padilla, E. Cerdeiras, L. Mestres, *J. Alloys Compd.* 726 (2017) 796–802. DOI: [10.1016/j.jallcom.2017.07.283](https://doi.org/10.1016/j.jallcom.2017.07.283)
- [2]. J. Lin, Y. Huang, Y. Bando, C. Tang, D. Golberg, *Chem. Commun.* 43 (2009) 6631–6633. DOI: [10.1039/b911215d](https://doi.org/10.1039/b911215d)
- [3]. Y. Ren, Y. Liu, S. Hao, H. Cui, H. Zhang, S. Meng, H. Ding, *Materials Science* 25 (2019) 7–12. DOI: [10.5755/j01.ms.25.1.19032](https://doi.org/10.5755/j01.ms.25.1.19032)
- [4]. J. Ding, Y. Li, Q. Wu, Q. Long, C. Wang, Y. Wang, *J. Mater. Chem. C* 3 (2015) 8542–8549. DOI: [10.1039/C5TC01508A](https://doi.org/10.1039/C5TC01508A)
- [5]. Quentin le Masne de Chermont, C. Chanéac, J. Seguin, F. Pellé, S. Maîtrejean, J.-P. Jolivet, D. Gourier, M. Bessodes, D. Scherman, *PNAS* 104 (2007) 9266–9271. DOI: [10.1073/pnas.0702427104](https://doi.org/10.1073/pnas.0702427104)
- [6]. J. Lee, S. Cho, *J. Nanosci.* 17 (2017) 7723–7728. DOI: [10.1166/jnn.2017.14836](https://doi.org/10.1166/jnn.2017.14836)
- [7]. L. Kovba, L. Lykova, V. Balashov, *Russ. J. Inorg. Chem.* 30 (1985) 311 (in Russian).
- [8]. V.F. Zolin, S.N. Vetkina, V.M. Markushev, *Sov. J. Quantum Electron.* 18 (1988) 204–206. DOI: [10.1070/QE1988v018n02ABEH011475](https://doi.org/10.1070/QE1988v018n02ABEH011475)
- [9]. E. Bernardo, *J. Non-Cryst. Solids* 354 (2008) 3486–3490. DOI: [10.1016/j.jnoncrysol.2008.03.021](https://doi.org/10.1016/j.jnoncrysol.2008.03.021)
- [10]. J. Faber, T. Fawcett, *Acta Cryst. B* 58 (2002) 325–332. DOI: [10.1107/S0108768102003312](https://doi.org/10.1107/S0108768102003312)
- [11]. J. Rodríguez-Carvajal, *Physica B* 192 (1993) 55–69. DOI: [10.1016/0921-4526\(93\)90108-I](https://doi.org/10.1016/0921-4526(93)90108-I)
- [12]. W. Kraus, G. Nolze, *J. Appl. Cryst.* 29 (1996) 301–303. DOI: [10.1107/S0021889895014920](https://doi.org/10.1107/S0021889895014920)
- [13]. M.R. Bissengaliyeva, D.B. Gogol, S.T. Taymasova, N.S. Bekturganov, *J. Chem. Eng. Data* 56 (2011) 195–204. DOI: [10.1021/je100658y](https://doi.org/10.1021/je100658y)
- [14]. W.T. Fu, D.J.W. IJdo, A. Bontenbal, *J. Solid State Chem.* 201 (2013) 128–132. DOI: [10.1016/j.jssc.2013.01.042](https://doi.org/10.1016/j.jssc.2013.01.042)
- [15]. H. Mons, M. Schriewer, W. Jeitschko, *J. Solid State Chem.* 99 (1992) 149–157. DOI: [10.1016/0022-4596\(92\)90299-B](https://doi.org/10.1016/0022-4596(92)90299-B)
- [16]. B.H. Justice, E.F. Westrum Jr., *J. Phys. Chem.* 67 (1963) 339–345. DOI: [10.1021/j100796a031](https://doi.org/10.1021/j100796a031)
- [17]. B.H. Justice, E.F. Westrum Jr., *J. Phys. Chem.* 67 (1963) 345–351. DOI: [10.1021/j100796a032](https://doi.org/10.1021/j100796a032)
- [18]. E. Gmelin, *Verlag der Zeitschrift für Naturforschung* 24 (1969) 1794–1800. DOI: [10.1515/zna-1969-1120](https://doi.org/10.1515/zna-1969-1120)
- [19]. P. Goel, M.K. Gupta, R. Mittal, S. Rols, S.N. Achary, A.K. Tyagi, S.L. Chaplot, *Phys. Rev. B* 91 (2015) 094304. DOI: [10.1103/PhysRevB.91.094304](https://doi.org/10.1103/PhysRevB.91.094304)
- [20]. A.E. Musikhin, M.A. Bespyatov, V.N. Shlegel, O.E. Safonova, *J. Alloys Compd.* 802 (2019) 235–243. DOI: [10.1016/j.jallcom.2019.06.197](https://doi.org/10.1016/j.jallcom.2019.06.197)
- [21]. M.R. Bissengaliyeva, R.M. Zhakupov, A.V. Knyazev, D.B. Gogol, Sh.T. Taimassova, B.K. Balbekova, N.S. Bekturganov, *J. Therm. Anal. Calorim.* 142 (2020) 2287–2301. DOI: [10.1007/s10973-020-09315-5](https://doi.org/10.1007/s10973-020-09315-5)
- [22]. M.R. Bissengaliyeva, M.A. Bespyatov, D.B. Gogol, *J. Chem. Eng. Data* 55 (2010) 2974–2979. DOI: [10.1021/je901040d](https://doi.org/10.1021/je901040d)
- [23]. M.A. Bespyatov, V.N. Naumov, *Bull. Kazan Technol. Univ. [Vestnik Kazanskogo Tehnologicheskogo Universiteta]* 1 (2010) 33–36 (in Russian).
- [24]. G.A. Krestov, K.B. Yatsimirskii, *Russ. J. Inorg. Chem.* 6 (1961) 1165–1169 (in Russian).
- [25]. T.P. Melia, R.J. Merrifield, *J. Inorg. Nucl. Chem.* 32 (1970) 2573–2579. DOI: [10.1016/0022-1902\(70\)80304-9](https://doi.org/10.1016/0022-1902(70)80304-9)